

A long-term dataset of simulated epilimnion and hypolimnion temperatures in 401 French lakes (1959-2020)

Najwa Sharaf^{1,2}, Jordi Prats³, Nathalie Reynaud^{1,2}, Thierry Tormos^{1,4}, Rosalie Bruel^{1,4},
Tiphaine Peroux^{1,2}, Pierre-Alain Danis^{1,4}

¹Pôle R&D Ecosystèmes Lacustres (ECLA), OFB-INRAE-USMB, Aix-en-Provence, France

²INRAE, Aix Marseille Univ, RECOVER, Team FRESHCO, 3275 Route Cézanne, 13182 Aix-en-Provence, France

³SEGULA Technologies, C. Calàbria 169, 08015 Barcelona, Spain

⁴OFB, Service ECOAQUA, DRAS, 3275 Route Cézanne, 13100 Aix-en-Provence, France

Correspondence to: Sharaf Najwa (najwa.sharaf@inrae.fr), Bruel Rosalie (rosalie.brue@ofb.gouv.fr), Tormos Thierry (thierry.tormos@ofb.gouv.fr), Reynaud Nathalie (nathalie.reynaud@inrae.fr)

54 **1. Abstract**

55 Understanding the thermal behavior of lakes is crucial for water quality management. Under climate change, lakes
56 are warming and undergoing alterations in their thermal structure, including surface and deep-water temperatures.
57 These changes require continuous monitoring due to the possible major ecological implications on water quality
58 and lake processes. We combined numerical modelling and satellite thermal data to create a regional dataset
59 (LakeTSim: Lake Temperature Simulations) of long-term water temperatures for 401 French lakes in order to
60 tackle the scarcity of in situ water temperature. The dataset consists of daily epilimnion and hypolimnion water
61 temperatures for the period 1959-2020 simulated with the semi-empirical OKPLM (Ottosson-Kettle-Prats Lake
62 Model) and the associated uncertainties. Here, we describe the model and its performance. Additionally, we present
63 the uncertainty analysis of simulations with default parameter values (parametrized as a function of lake
64 characteristics) and calibrated parameter values, along with the analysis of the sensitivity of the model to parameter
65 values and biases in the input data. Overall, the 90% confidence uncertainty range is largest for hypolimnion
66 temperature simulations with a median of 8.5 °C and 2.32 °C respectively with default and calibrated parameter
67 values. There is less uncertainty associated with epilimnion temperature simulations with a median of 5.42 °C and
68 1.85 °C, respectively before and after parameter calibration. This dataset provides over six decades of epilimnion
69 and hypolimnion temperature data, crucial for climate change studies at a regional scale. It will help provide insight
70 into the thermal functioning of French lakes and can be used to help decision-making and stakeholders.

71 **2. Introduction**

72 Lakes, both natural and artificial (i.e., reservoirs and gravel pits) are sentinels of environmental change and provide
73 important services such as access to drinking water, hydropower production, recreation and fisheries (Adrian et
74 al., 2009). Under climate change and anthropogenic pressures, many lakes are warming and consequently
75 experiencing changes to their biophysicochemical structure and function that are leading to services being
76 compromised (Janssen et al., 2021).

77 In lakes, water temperature is an essential parameter regulating processes such as the functioning of trophic webs,
78 oxygen conditions, the physical structure of the water column as well as the biogeochemistry (Yang et al., 2018).
79 Under warming, historical records and future projections demonstrate that for lakes, alterations in the
80 thermodynamic functioning including warmer temperatures and shifts in mixing regimes already took place and
81 are expected to persist in the future (Shatwell et al., 2019; Woolway and Merchant, 2019). In this context, they are
82 undergoing shorter periods of ice cover and longer, more stable periods of thermal stratification (Woolway et al.,
83 2022). These alterations could have considerable ecological implications for the biological communities (Lind et
84 al., 2022; Havens and Jeppesen, 2018). For instance, worldwide studies have shown that the expansion of toxic
85 cyanobacterial blooms is linked to warming (Griffith and Gobler, 2020). Other responses include species reduced
86 body size (Daufresne et al., 2009), changes in thermal habitat and shifts in species seasonality (Kharouba et al.,
87 2018).

88 It is thus crucial to closely evaluate water temperature trajectories over the entire water column in space and time
89 when assessing the impact of climate change on lake ecosystems. However, the lack of data coverage, both
90 spatially and temporally, makes it difficult to accurately characterize lakes thermal response to climate change and
91 to identify warming trends (Gray et al., 2018). Indeed, long-term datasets of in situ temperatures are usually scarce
92 and mostly limited to large lakes (Layden et al., 2015). Moreover, sampling frequency and temporal coverage of

93 in situ water temperature varies greatly from one lake to the next, from a few years (Sharma et al., 2015) up to
94 decades (Piccolroaz et al., 2020; Rimet et al., 2020).

95 Due to the difficulties in conventional in situ monitoring, often expensive, the coupling of modelling and satellite
96 remote sensing data has become fundamental in the field of limnology (Nouchi et al., 2019). Modelling provides
97 means to interpolate both temporal and spatial gaps. It thereby allows us to acquire information about surface water
98 temperatures, which are globally the focus of lake climate change studies, and deep-water temperatures which are
99 as critical though often disregarded in this context. Several numerical models that vary in complexity exist for
100 conducting water temperature simulations, the most accurate being deterministic or process-based models.
101 Nevertheless, regional or global deterministic modelling efforts over long periods are usually hindered by the lack
102 of sufficiently detailed input data (e.g., meteorological and field data) to run the models (Kim et al., 2021). For
103 practical and operational purposes, simpler models (semi-empirical, statistical or hybrid physical-statistical based
104 models) with less requirements for forcing data, have been mostly applied to assess the impact of climate change
105 on lake ecosystems and study them (Piccolroaz et al., 2020; Toffolon et al., 2014; Sharma et al., 2008). Long-term
106 simulations across a considerable number of lakes are made possible with this type of models, enabling the
107 detection of trends in time series data that are not achievable with shorter datasets (Gray et al., 2018).

108 The performance of numerical models depends highly on the calibration of their parameters as well as on the
109 quality of the input data. Satellite remote sensing is an effective way to monitor surface water temperature on a
110 synoptic scale (Schaeffer et al., 2018; Sharaf et al., 2019) and provide a complementary source of data to in situ
111 measurements for model calibration or validation purposes (Allan et al., 2016; Babbar-Sebens et al., 2013). In
112 particular, thermal infrared sensors onboard the Landsat satellites are very adequate for retrospective analysis of
113 surface water temperature with a spatial resolution adapted for small to medium size lakes and reservoirs at a
114 bimonthly acquisition frequency. Landsat 4 and 5 TM (Thematic Mapper), 7 ETM+ (Enhanced Thematic Mapper)
115 and 8 TIRS (Thermal InfraRed Sensor) provide surface temperature data at spatial resolutions of 120, 60 and 100
116 m respectively. Landsat series records of surface water temperature can be used to validate 3D hydrodynamic
117 models when in situ measurements are scarce (Sharaf et al., 2021) and to spatially assess the quality and suitability
118 of aquatic habitat for biological communities (Halverson et al., 2022). Although, satellite thermal data is limited
119 to the surface, its integration into model calibration could improve the accuracy of simulations over the surface
120 layer and the water column (Javaheri et al., 2016).

121 Here we present on a regional scale, a long-term dataset, LakeTSim (Lake Temperature Simulations), of daily
122 epilimnion and hypolimnion temperature simulations, as well as uncertainties, for the period 1959-2020 over 401
123 French lakes monitored under the Water Framework Directive (WFD) including natural and artificial lakes,
124 reservoirs and gravel pits. We present the OKPLM (Ottosson-Kettle-Prats Lake Model) used to produce water
125 temperature simulations and its performance. Further, we provide the uncertainty analysis of simulations with
126 default (parametrized with satellite thermal data over an entire set of lakes) and calibrated (with in situ temperature
127 measurements for each lake) model parameter values as well as the sensitivity analysis for the latter. The goal of
128 publishing this dataset is to provide new insight about epi- and hypolimnion temperatures of lakes in France
129 especially for those that are not monitored regularly through conventional methods. This long-term dataset is
130 valuable for developing temperature indicators for identifying warming trends, extreme events and possible

131 changes in the mixing regime among others. These indicators will contribute to assess the impact of climate change
132 on lakes thermal functioning and its influence on the biological community structure and trophic webs.

133 **3. Data and methodology**

134 **3.1. The software suite ALAMODE**

135 The simulations, sensitivity and uncertainty analysis presented in this paper were made using the software suite
136 ALAMODE (A LAke MODElling project). ALAMODE (Danis, 2020) is a software suite developed in Python 3
137 by the Pôle R&D Ecosystèmes Lacustres (ECLA) and SEGULA Technologies to facilitate the realization of
138 simulations of lakes and the management of related information. It comprises multiple modules and packages
139 designed for lake and tributary modelling, as well as for processing the data necessary to operate these models.
140 These packages include OKPLM (Ottosson-Kettle-Prats Lake Model), CUSPY (Calibration, Uncertainty analysis
141 and Sensitivity analysis in PYthon), TMOD (Temperature MODelling), GLMtools (General Lake Model tools),
142 “tributary”, TINDIC (Temperature INDICators) and ALAPROD (ALAMODE-Production). OKPLM (Prats-
143 Rodríguez and Danis, 2023b) is used to simulate epilimnion and hypolimnion water temperatures in lakes while
144 CUSPY (Prats-Rodríguez and Danis, 2023a) is used for model parameters estimations and conducting uncertainty
145 and sensitivity analyses. TMOD is used for managing the T-MOD database designated to facilitate the realization
146 and consultation of simulations. GLMtools is used to conduct lake hydrodynamic simulations using the one-
147 dimensional hydrodynamic General Lake Model (Hipsey et al., 2019) while “tributary” is used for the estimation
148 of flow and temperature of lake tributaries. The package TINDIC is used for calculating temperature indicators
149 from model simulations. Finally, ALAPROD integrates all the functionalities to produce simulations into a single
150 package: simulation of stream water temperature, of lake hydrodynamics and temperature, and of stream flow rate.
151 It also includes sensitivity and uncertainty analysis features. The functionalities of these packages can be accessed
152 either by using each package separately or by utilizing the ALAPROD package, which depends on the TMOD
153 database and requires access to it.

154 At present, only the ALAMODE packages related to the main functionalities used in this work are publicly
155 available (see Code availability section): the simulation of lake temperatures using the Ottosson-Kettle-Prats Lake
156 Model (Prats & Danis, 2019), implemented in the package OKPLM, and the sensitivity and uncertainty analysis
157 tools in the CUSPY package. We used ALAPROD to access the functionalities of both packages.

158 **3.2. The OKP Lake Model description**

159 The OKPLM (Ottosson-Kettle-Prats Lake Model) (Prats & Danis, 2019) is a two-layer semi-empirical data model
160 adapted from Kettle et al (2004) for the epilimnion module and Ottosson & Abrahamsson (1998) for the
161 hypolimnion module. The modifications proposed in Prats & Danis (2019) consisted mainly of simplifying the
162 mixing algorithm used in Ottosson & Abrahamsson (1998) using a basic stability condition, whereas for the
163 epilimnion module a sinusoidal fit to average daily solar radiation was used instead of the theoretical clear-sky
164 radiation. The OKPLM also runs on weekly and monthly frequencies. The regionalization of the parameters of the
165 model mainly depends on the geographical and morphological properties of the lake (maximal depth, volume,
166 surface area, latitude and altitude). The model requires few meteorological forcing data: solar radiation and air
167 temperature.

168 The model calculates water temperature as follows:

169 $T_{e,i} = A + Bf(T_{a,i}^*) + CS_i$ (1)

170 where T_e is the epilimnion temperature (°C), i is the day number, A , B and C are calibration parameters, S is the
171 solar radiation (W m^{-2}) and $f(*)$ is an exponential smoothing function with $T_{a,i}^*$ defined as:

172 $T_{a,i}^* = T_{a,i} - MAAT$ (2)

173 Where $T_{a,i}$ is air temperature (°C) and $MAAT$ is the annual mean air temperature (°C). The smoothing function
174 $f(*)$ is such that it gives greater weight to the nearest observations and the weights decrease exponentially. It is
175 defined as:

176 $f(T_{a,1}^*) = T_{a,1}^*$ (3)

177 $f(T_{a,i}^*) = \alpha T_{a,i}^* + (1 - \alpha)f(T_{a,i-1}^*)$ (4)

178 where α is the smoothing factor. When $\alpha = 1$ there is no smoothing, while the smoothing increases with the
179 decrease in the value of α .

180 $T_{h,i} = A \cdot D + E \cdot g(T_{e,i})$ (5)

181 where T_h is the hypolimnion temperature (°C), D and E are calibration parameters and $g(T_{e,i})$ is an exponential
182 smoothing as follows:

183 $g(T_{e,1}) = T_{e,1}$ (6)

184 $g(T_{e,i}) = \beta T_{e,i} + (1 - \beta)g(T_{e,i-1})$ (7)

185 where β is the exponential smoothing factor. As for α , there is no smoothing for $\beta = 1$ and the smoothing increases
186 as β approaches zero.

187 In ALAPROD, OKPLM can be run in two modes: the “default” mode where model parameter values for each
188 lake are estimated using the parameterization presented in Prats & Danis (2019), and the “calibrated” mode where
189 model parameters are calibrated individually for each lake by using in situ temperature measurements. The default
190 parameterization was obtained by using the individually calibrated parameter values to fit appropriate expressions
191 as a function of the characteristics of lakes. In the epilimnion module model parameter values A , B , C , and α are
192 estimated based on lake characteristics (i.e., latitude, altitude, surface area, volume, and depth). These equations
193 were determined using robust regressions and Landsat infrared data from 1999 to 2016 of French lakes to estimate
194 surface temperatures (Prats et al., 2018). In contrast, for the hypolimnion module, parameter values E and β were
195 derived as a function of lake depth and lake type using temperature profile data from 357 lakes; β can have a value
196 of 1 ($E > 0.95$) or 0.13 ($E \leq 0.95$). The parameter D was assigned a constant value of 0.51.

197 The parametrization of the OKPLM parameters as presented in Prats & Danis (2019) is as follows:

198 $A = 39.9 - 0.484L_{Lat} - 4.52 \times 10^{-3}L_{Alt} - 0.167\ln L_A$ (8)

199 where L_{Lat} is lake latitude (°N), L_{Alt} is lake altitude (m) and L_A is lake surface area (m^2).

200 $B = 1.058 - 0.0010L_{Dmax}$ (9)

201 where L_{Dmax} is lake maximal depth (m).

$$202 \quad C = 1.12 \times 10^{-3} - 3.62 \times 10^{-6} L_{Alt} \quad (10)$$

$$203 \quad E = e_1 + \frac{1-e_1}{1+\exp[e_3(e_2-\ln L_D)]} \quad (11)$$

204 where e_1 , e_2 and e_3 are coefficients with respective values of 0.10, 2.0, -1.8 for natural lakes and 0.49, 1.7, -2.0
205 for artificial lakes (reservoirs, gravel pits, ponds and quarry lakes) and L_D is lake mean depth (m).

$$206 \quad \alpha = \exp(0.52 - 3.0 \times 10^{-4} L_{Alt} + 0.25 \ln L_A - 0.36 \ln L_V) \quad (12)$$

207 where L_V is lake volume (m³).

208 **3.3. Input data**

209 The OKPLM was forced with two sources of meteorological data extracted from the SAFRAN (Système d'Analyse
210 Fournissant des Renseignements Adaptés à la Nivologie) analysis system (Durand et al., 1993) and the S2M
211 (SAFRAN–SURFEX/ISBA–Crocus–MEPRA) meteorological reanalysis (Vernay et al., 2015, 2022).

212 The SAFRAN system provides meteorological variables at an hourly time step estimated through interpolation
213 and assimilation processes with an 8 km square grid. Average daily data from the nearest grid cell was selected
214 for each study site. The difference in altitude between the study site and the grid cell was accounted for by applying
215 an adiabatic elevation correction on air temperature.

216 The S2M model chain combines the SAFRAN meteorological analysis and the SURFEX/ISBA–Crocus snow
217 cover model including MEPRA (Modèle Expert d'Aide à la Prévision du Risque d'Avalanche). It is more adapted
218 to mountainous regions as it has a spatial definition where spatial heterogeneity is taken into consideration. The
219 S2M reanalysis uses a vertical resolution of 300 m and is the result of simulations performed over mountainous
220 zones referred to as “massifs” and covering the French Alps, Pyrenees and Corsica mountainous regions. In order
221 to use S2M meteorological data over each lake an extraction of certain topographic classes is necessary. These
222 include elevation, aspect and slope, which represent the spatial variability over “massifs”. On average, a massif
223 corresponds to a mountainous region of about 1000 km² over which meteorological conditions are considered
224 homogeneous at a given elevation range. Two types of S2M reanalysis simulations exist for each elevation range,
225 one at flat terrain and the other with 8 aspects at 2 different slope angles. For this study, this information (elevation,
226 slope, aspect) was extracted from a Digital Elevation Model (BD Alti, IGN) for each lake over its drainage basin,
227 combined into zones corresponding to S2M topographic classes. We considered a zero slope and average daily
228 data for each study site.

229 In situ temperature profiles, geographical and morphological data of the study sites were initially extracted from
230 the PLAN_DEAU database. The extracted data was then incorporated into the T-MOD database, with the aim of
231 simplifying the process of simulations and accessing information about the characteristics of the simulated lakes.
232 Both databases are managed by INRAE (l'Institut National de Recherche pour l'Agriculture, l'Alimentation et
233 l'Environnement) and Pôle R&D ECLA ("ECosystèmes Lacustres") in Aix-en-Provence, France. The
234 geomorphological data consisting of maximal depth, volume, surface area, latitude and altitude were extracted for
235 401 lakes. In situ temperature profiles were extracted for 170 lakes over different depths. Depending on each lake,

236 the number of years with samples could vary from 1 to 12 with a number of samples ranging between 1 and 10 per
237 year.

238 **3.4. Lake simulations**

239 For this study, we considered 401 lakes (Figure 1) located in Metropolitan France monitored according to the
240 Water Framework Directive (WFD). Here we refer to lakes as natural lakes, reservoirs, gravel pits and other
241 artificial lakes (e.g., ponds and quarry lakes). The present lake dataset includes epi- and hypolimnion temperature
242 simulations for 54 natural lakes, 302 reservoirs, 7 gravel pits and 38 other artificial lakes (Figure 2). The lakes
243 characteristics range between 0 and 2279.7 m for altitude, 0.8 and 309.7 m for maximal depth, 0.08 and 577.12
244 km² for surface area and 5×10^4 and 8.9×10^{10} m³ for volume.

245 The OKPLM was run using “default” and “calibrated” parameters with two sources of meteorological data,
246 SAFRAN and S2M over specific sets of lakes. “Calibrated” model parameters were adopted when in situ
247 temperature measurements were available; conversely, “default” parameters were used. S2M data are more
248 representative of mountainous meteorological conditions than SAFRAN data and were thus used, when possible,
249 for simulating the water temperature in lakes situated at altitudes higher than 900 m. For some lakes, it was not
250 possible to use S2M data, either because their drainage basins are not entirely part of a massif ($n = 1$), or because
251 they are located in massifs that are not covered by the S2M reanalysis dataset ($n = 18$). Among the total number
252 of study sites ($n = 401$), the model was forced using SAFRAN and S2M meteorological data respectively for 210
253 and 21 lakes with “default” model parameters, and for 164 and 6 lakes with “calibrated” model parameters. The
254 geomorphological characteristics of the simulated lakes with each of the abovementioned configurations are shown
255 in Table 1.

256

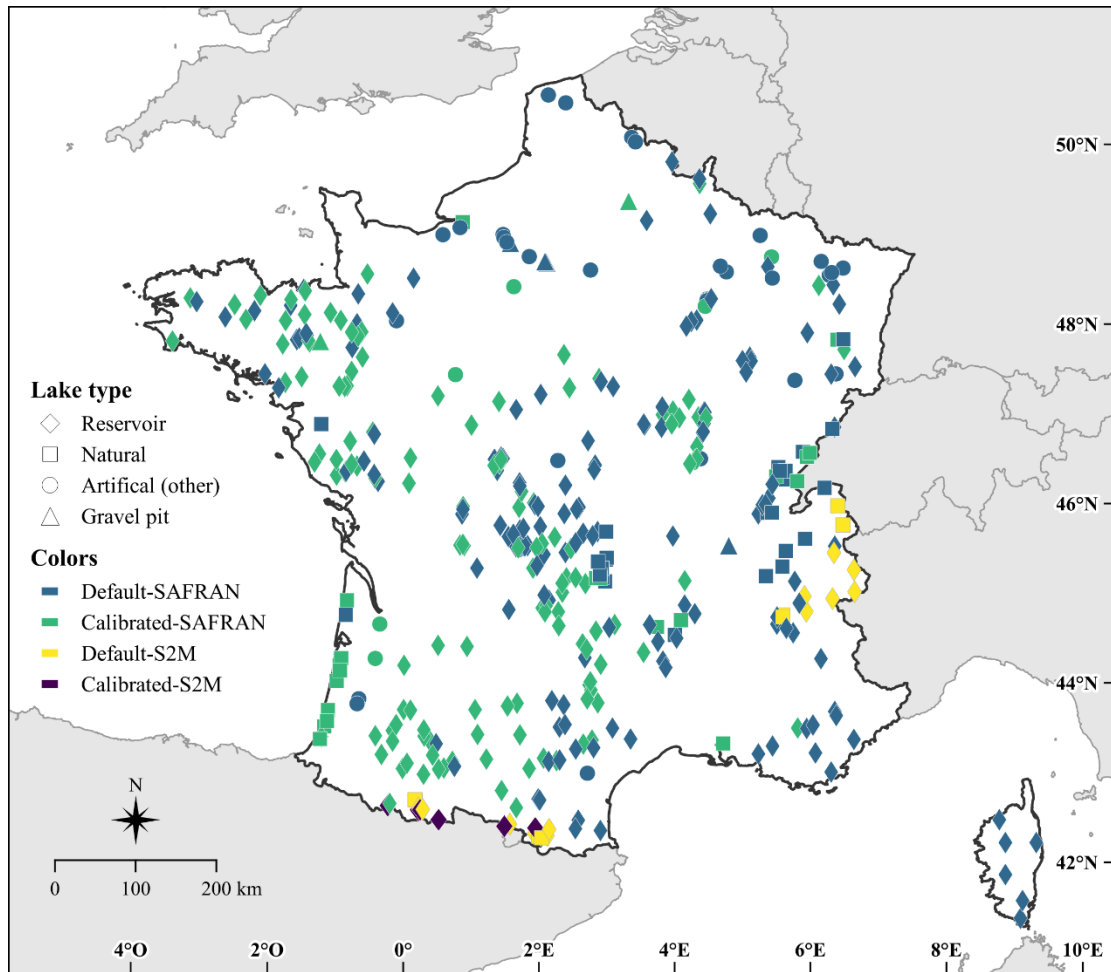


Figure 1: Location and lake type of the 401 French lakes simulated with the OKPLM in “default” and “calibrated” modes, with SAFRAN and S2M meteorological data for the period 1959-2020.

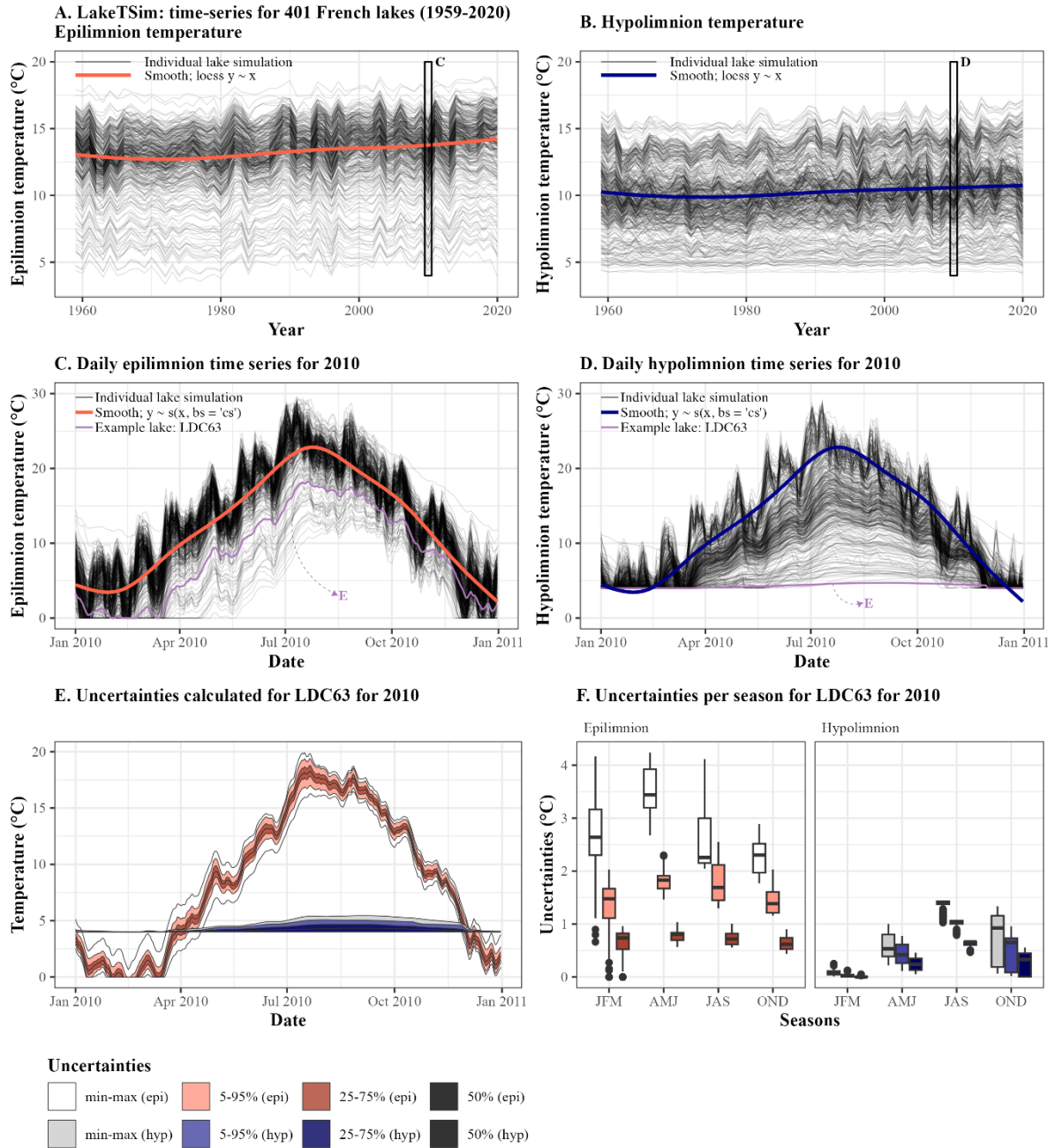


Figure 2: Presentation of the LakeTSim data. (A) Epilimnion and (B) hypolimnion mean annual temperatures, with average trend across lakes shown with a smooth spline. (C) Daily epilimnion temperature per lake in the dataset for 2010, with smooth spline and the time series for one lake (LDC63) highlighted. (D) Daily hypolimnion temperature per lake in the dataset for 2010, with smooth spline and the time series for one lake (LDC63) highlighted. LDC63 is the code for Lake Chauvet, a natural lake (45.46 °N, 2.83 °E) located at 1167 m asl, with a surface area of 0.51 km², a volume of 17.41 10⁶ m³, and a maximum depth of 66.8 m. The simulation for LDC63 was conducted resorting to SAFRAN data and was run with the “calibrated” mode. (E) Uncertainties were calculated per lake and per day and are shown here daily for LDC63, in 2010, for both the epilimnion (epi) and the hypolimnion (hyp). (F) Uncertainties are shown here seasonally for LDC63, in 2010, for both the epilimnion (epi) and the hypolimnion (hyp). JFM corresponds to January-February-March, AMJ corresponds to April-May-June, JAS corresponds to July-August-September and OND corresponds to October-November-December.

Table 1: Characteristics of the lakes simulated with the OKPLM in “default” and “calibrated” modes with SAFRAN and S2M meteorological data for the period 1959-2020; n represents the number of lakes.

Variables	Minimal - Maximal range			
Model parameters	Default		Calibrated	
Meteorological data	SAFRAN	S2M	SAFRAN	S2M
n	210	21	164	6
Altitude (m)	1 - 1753	916 - 2213	0 - 2279.7	1577.5 - 2172.5
Latitude (°N)	41.47 - 50.87	42.55 - 46.21	42.88 - 49.87	42.65 - 42.86
Longitude (°E)	-3.90 - 9.48	0.08 - 6.94	-4.24 - 6.96	-0.33 - 1.92
Maximal depth (m)	0.8 - 309.7	10.3 - 180	1.2 - 124	49 - 112
Surface area (km ²)	0.08 - 577.12	0.11 - 6.52	0.29 - 57.57	0.45 - 1.21
Volume (m ³)	$5 \times 10^4 - 8.9 \times 10^{10}$	$51.4 \times 10^4 - 33.32 \times 10^7$	$12.9 \times 10^4 - 49.88 \times 10^7$	$72.7 \times 10^5 - 68.6 \times 10^6$

258

259 3.5. Calibration, uncertainty and sensitivity analysis

260 Calibration, uncertainty and sensitivity analyses were carried out using the package “CUSPY” (Calibration,
 261 Uncertainty analysis and Sensitivity analysis in PYthon), which is part of the software suite “ALAMODE” (Danis,
 262 2020) and acts as an interface to the package “pyemu” (White et al., 2016, 2020).

263 Parameter values were calibrated for lakes with enough available in situ data (temperature profiles and
 264 bathymetry). Parameter values were calibrated using the Gauss-Levenberg-Marquardt algorithm and Tikhonov
 265 regularization (White et al., 2020), and the squared sum of residuals as objective function. In addition to the
 266 calibrated parameter values, the calibration process also provided posterior parameter uncertainty and composite
 267 scaled sensitivities. Composite scaled sensitivities (CSS) indicate the quantity of information provided by each
 268 parameter and the sensitivity of the model to them (Ely, 2006). The parameters with higher CSS values will have
 269 a greater impact on the resulting simulation compared to those with low CSS values. To determine the CSS values
 270 for each parameter, the Dimensionless Scaled Sensitivities (DSS) are used. DSS indicate how important an
 271 observation or how sensitive a simulated equivalent of an observation is in relation to the estimation of a parameter.
 272 Further information on these statistical measures is available in Hill (1998) and Poeter & Hill (1997). The
 273 dimensionless scaled sensitivity for i and j , i being one of the observations and j being one of the parameters, is
 274 calculated as:

$$275 \quad DSS_{i,j} = \left[\frac{\partial y'_i}{\partial b_j} \right] b_j w_i^{1/2} \quad (13)$$

276 where y'_i is the simulated value associated with the i th observation, b_j is the j th estimated parameter, $\frac{\partial y'_i}{\partial b_j}$ is the
 277 sensitivity of the simulated value associated with the i th observation and w_i is the weight of the i th observation.

278 The CSS for parameter j is calculated from DSS as follows:

$$CSS_j = \left[\frac{\sum_{i=1}^{ND} (DSS_{ij})^2 |b|}{ND} \right]^{1/2} \quad (14)$$

where ND is the number of observations and \mathbf{b} is a vector of parameters values.

The uncertainty of the simulations (calibrated and default) was analyzed using Monte Carlo simulations. For each lake, 100 Monte Carlo simulations were carried by randomly selecting the value of the model parameters. Two parameters, *at_factor* and *sw_factor*, multiplying the meteorological input, were added to account for possible uncertainties in input data. For default simulations, the a priori distribution of the parameters was assumed to follow a normal distribution with the average value and lower and upper bounds shown in Table 2. The ranges for parameters A , B and C were estimated as four times the standard deviation of the residuals of the formulas used to estimate them according to Prats & Danis (2019). The parameters D , E and β , are expected to lie in the range 0-1 for mathematical and physical reasons. However, their respective values are highly interdependent and are difficult to identify. Given their higher uncertainty, the full 0-1 range was explored. For *MAAT*, *at_factor* and *sw_factor*, reasonable ranges ($\pm 10\%$) were chosen to account for meteorological data uncertainty (measurement error, errors in regionalization, etc.). For calibrated simulations, the distribution of the parameters was obtained from the calibration results.

In this study, the non-parametric Kendall's tau coefficient (significance level at 5%) was used to identify statistical associations between uncertainty values and *CSS* in respect to lake geomorphological characteristics (maximal depth, volume, surface area, latitude and altitude).

Table 2: Characteristics of the a priori distributions of the model parameters. Parameters with a circumflex accent indicate parameter values estimated for a particular lake according to the regionalization formulas by Prats & Danis (2019).

Parameter	Average value	Lower bound	Upper bound
A	\hat{A}	$\hat{A} - 2 \cdot 0.74$	$\hat{A} + 2 \cdot 0.74$
B	\hat{B}	$\hat{B} - 2 \cdot 0.08$	$\hat{B} + 2 \cdot 0.08$
C	\hat{C}	$\hat{C} - 2 \cdot 0.004$	$\hat{C} + 2 \cdot 0.004$
D	\hat{D}	0	1
E	\hat{E}	0	1
α	$\hat{\alpha}$	0	$\hat{\alpha} + 2 \cdot 0.08$
β	$\hat{\beta}$	0	1
<i>MAAT</i>	$M\hat{A}AT$	$M\hat{A}AT - 2 \cdot 0.5$	$M\hat{A}AT + 2 \cdot 0.5$
<i>at_factor</i>	1	0.9	1.1
<i>sw_factor</i>	1	0.9	1.1

296

297 **4. Model performance**

298 The performance of the OKPLM was assessed in Prats & Danis (2019) by comparing its performance to two other
299 often-applied models in lake studies, air2water and FLake. The air2water model is a semi-empirical model used
300 to calculate the epilimnion temperature of temperate lakes (Toffolon et al., 2014; Piccolroaz et al., 2013). FLake
301 is a one-dimensional (1D) hydrodynamic lake model for simulating temperature vertical profiles and mixing
302 conditions in lakes (Mironov, 2008). To assess their performances, the three models were run between 1999 and
303 2016 over two sets of French lakes of different types (reservoirs, natural lakes, ponds, quarry lakes and gravel
304 pits): a group of five lakes with continuous profile measurements, and a group of 404 lakes with less frequent
305 temperature measurements. The performance assessment was limited to the period of 1999-2016 due to the
306 availability of water temperature data (in situ and satellite) during that specific timeframe. The scarcity of in situ
307 water temperature measurements before 1999 applies to the entire set of lakes. However, it is important to note
308 that long-term in situ water temperature data is available for a few large lakes, which was used to assess the
309 performance of the three models (Prats & Danis, 2015). The OKPLM was run with the “default” parameter values
310 given by the parameterization in Prats & Danis (2019). The air2water parameter values were obtained as a function
311 of lake depth from the parametrization presented in Toffolon et al. (2014). When evaluating the model performance
312 with the set of five lakes with continuous data, air2water was also run using parameter values calibrated for the
313 individual lakes available data. FLake does not have calibration parameters. Meteorological- forcing (SAFRAN)
314 consisted of air temperature for the air2water model; solar radiation, vapor pressure, cloud cover and wind speed
315 for FLake; and air temperature and solar radiation for the OKPLM.

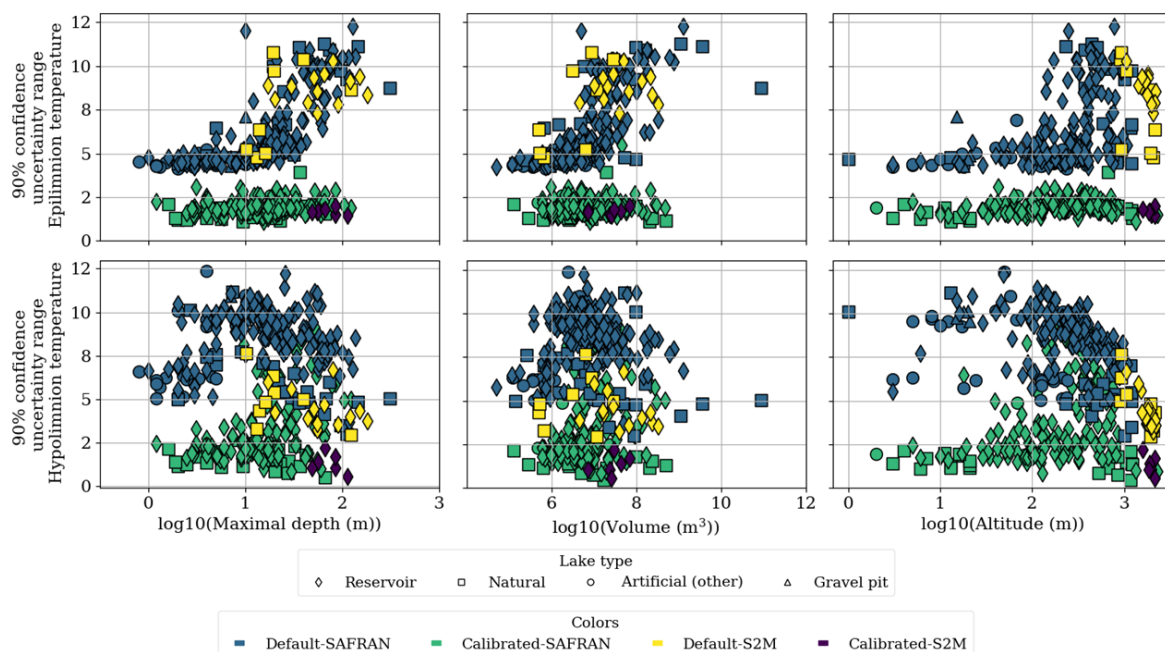
316 The OKPLM, air2water and FLake simulations were assessed through comparison to in situ measurements. For
317 epilimnion temperatures, the average discrepancies calculated between OKPLM simulations and observations
318 remained below 2 °C in most cases, in contrast to the air2water and Flake models. The performance comparison
319 between the OKPLM, air2water and FLake yielded respectively median RMSE's (Root Mean Square Error) of
320 1.7, 2.3 and 2.6 °C calculated between simulations and observations of epilimnion water temperature. Although
321 when using calibrated parameter values for air2water, median RMSE was below 1 °C in most cases. For
322 hypolimnion temperatures, the median RMSEs by lake type obtained with OKPLM simulations remained below
323 2 °C, except for gravel pits (RMSE = 2.7 °C) and reservoirs (RMSE = 2.3 °C), whereas FLake yielded a median
324 RMSE of 3.3 °C. For the epilimnion, the differences between the RMSE of lake types were not significant. In
325 terms of depth, discrepancies between epilimnion temperature simulations with the OKPLM and measurements
326 were highest for lakes with a depth > 10 m and for ponds around 1 m deep. The OKPLM simulations were also
327 evaluated seasonally, in particular during summer and winter. The model simulated temperatures well with a
328 median RMSE of 1.4 and 1.6 °C in summer and winter respectively.

329 **5. Uncertainty analysis**

330 Overall, for both simulations with default and calibrated model parameters, uncertainty was higher for
331 hypolimnion temperature compared to epilimnion temperature especially in reservoirs (Figure 3). In default
332 simulations, the uncertainty of simulated epilimnion temperatures showed a clear and strong relation with lake
333 maximal depth (Figure 3, Table 3). On one hand, maximal depth had the highest Kendall's tau value of 0.64 (p -
334 value < 0.0001), indicating a strong positive correlation with uncertainty followed by volume with a Kendall's tau
335 of 0.59 (p -value < 0.0001). Uncertainty increased with maximal depth and volume in particular for lakes with

336 depths greater than 10 m and volumes greater than 10^6 m^3 (Figure 3). Overall, lakes with higher maximal depths
 337 have higher volumes and are located at greater altitudes (Figures A1-A2 in Appendix A). On the other hand,
 338 moderate significant correlations were identified with surface area, altitude and latitude (Table 3). Lakes with
 339 larger surface areas and higher altitudes tend to have higher uncertainties whereas lakes located at higher latitudes
 340 tend to have lower uncertainties (Figure A3 in Appendix A). The latter can be linked to the fact that more shallow
 341 lakes are located at higher latitudes (Figure A1 in Appendix A). For default simulations of hypolimnion
 342 temperatures, uncertainty was maximal for lakes with depths around 10 m. Kendall's tau values revealed a
 343 moderate significant correlation between hypolimnion temperature uncertainty and altitude (-0.45 , p -value $<$
 344 0.0001). The decrease in uncertainties with altitude can be related to the fact that lakes situated at very high
 345 altitudes are mostly deep. Further, in the present dataset, lakes with higher maximal depths occur as altitude
 346 increases (Figure A1-A2 in Appendix A).

347 After calibration, there was an important reduction in simulation uncertainty. For default simulations of epilimnion
 348 temperature the median of the 90% confidence uncertainty range was $5.42 \text{ }^\circ\text{C}$, while after calibration it was 1.85
 349 $^\circ\text{C}$. For hypolimnion temperature, the median of the 90% confidence uncertainty range of default simulations was
 350 $8.5 \text{ }^\circ\text{C}$, while it was $2.32 \text{ }^\circ\text{C}$ after calibration. However, many reservoirs with depths greater than 8 m still had a
 351 much greater uncertainty (uncertainty range $> 4 \text{ }^\circ\text{C}$) than the rest of lakes after calibration. Additionally, reservoirs
 352 (and a few natural lakes) above 100 m in altitude showed the highest uncertainties in the simulation of epilimnion
 353 temperature.



354 **Figure 3: Average 90% confidence uncertainty range for epilimnion (top panel) and hypolimnion (bottom panel)**
 355 **temperatures in calibrated ($n = 170$) and default ($n = 231$) simulations for the period 1959-2020.**

355
 356

Table 3: Kendall's tau coefficients and p -values of average 90% confidence uncertainty range for epilimnion and hypolimnion temperatures obtained from default simulations (1959-2020) in respect to lakes geomorphological characteristics. For each lake, "Epilimnion uncertainty" and "Hypolimnion uncertainty" are defined as the average 90% confidence uncertainty range calculated as the difference between the 95th and 5th percentiles of the daily simulated epilimnion and hypolimnion water temperatures. The significance levels are represented as follows: *: $1.00e-02 < p\text{-value} \leq 5.00e-02$, **: $1.00e-03 < p\text{-value} \leq 1.00e-02$, *: $1.00e-04 < p\text{-value} \leq 1.00e-03$, ****: $p\text{-value} \leq 1.00e-04$. Otherwise, correlations are not significant ($p\text{-value} > 0.05$).**

	Maximal depth (m)	Surface area (km ²)	Altitude (m)	Latitude (°N)	Volume (m ³)
Epilimnion uncertainty	0.64****	0.31****	0.39****	-0.40****	0.59****
Hypolimnion uncertainty	-0.13**	0.05	-0.45****	0.03	-0.03

6. Sensitivity analysis

The parameter to which the model was most sensitive was the parameter C (Figure 4), which multiplies solar radiation in Eq. (1). The CSS for C were an order of magnitude greater than for the next parameters with highest CSS , the parameter α and at_factor , both influencing the effect of air temperature on simulated water temperature. Other parameters to which the model was somewhat sensitive were E , B and β . The model was quite insensitive to sw_factor , $MAAT$ and A . The parameter D , with CSS several orders of magnitude smaller than the other parameters, was unidentifiable.

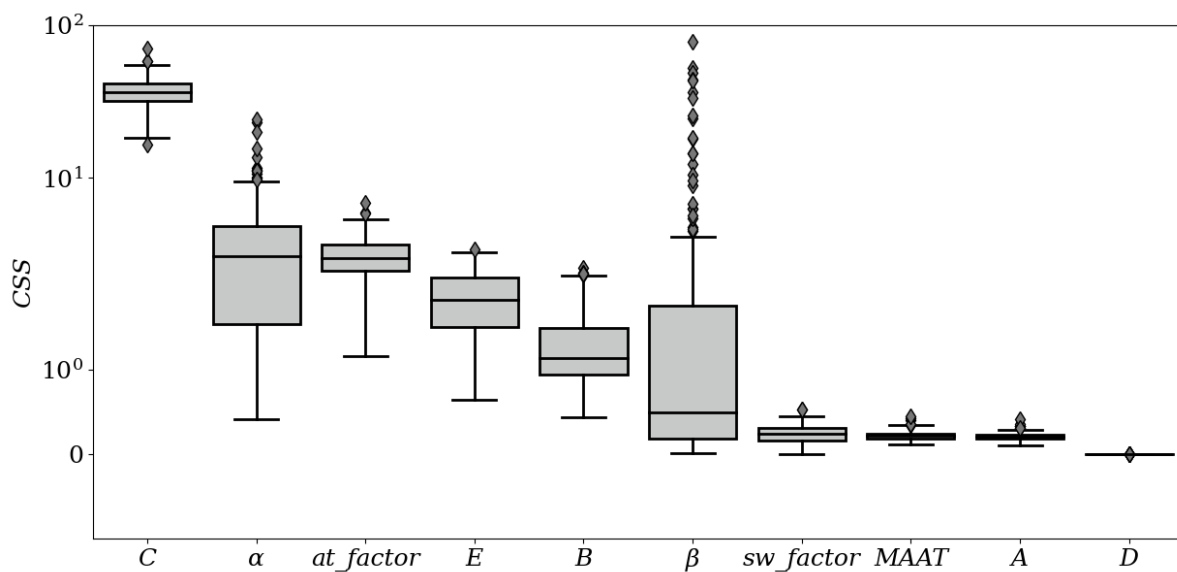


Figure 4: Composite scaled sensitivities (CSS) for each parameter. The boxplots indicate the distribution of CSS between the simulations calibrated for different lakes. The y-axis is in logarithmic form.

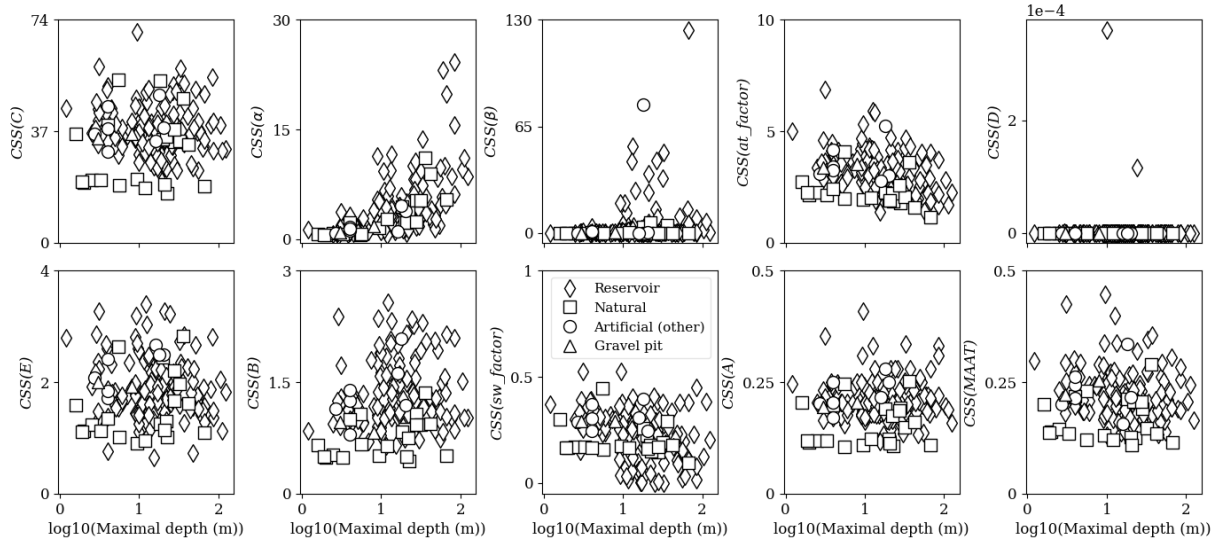
The model tended to be more sensitive to the parameter values in the case of reservoirs than in the case of natural lakes (Figure 5, Figures A4-A7 in Appendix A). Some parameters showed a dependency on lakes geomorphological characteristics. With the exception of a weak correlation with altitude (Kendall's tau = 0.18), there was no significant dependence between the parameter C and lakes geomorphological characteristics (Table 4, Figure A4 in Appendix A). The parameter α being parametrized as a function of lake volume, surface area and

371 altitude reflects the thermal inertia of the lake. It showed a clear highly significant dependency primarily on lake
 372 depth (Kendall's tau = 0.47) followed by altitude (Kendall's tau = 0.4) and volume (Kendall's tau = 0.39) (Figure
 373 5, Table 4). The increase of model sensitivity to the parameter α primarily with depth as well as altitude and volume
 374 propagated to the default simulations and explain the increased uncertainty with these same geomorphological
 375 characteristics in the default simulations. The parameter at_factor , was weakly but significantly correlated with
 376 all lakes geomorphological characteristics except for latitude with which no correlation was found (Figure 5, Table
 377 4, Figures A4-A7 in Appendix A). CSS were mostly low for the parameter β , except for a few reservoirs and
 378 artificial lakes that scored very high CSS values. The sensitivity of β displayed a weak but significant correlation
 379 with lakes geomorphological characteristics, except for volume (Table 4).

380 Although the model in general was not very sensitive to the values of the parameters most directly related with
 381 hypolimnion temperatures (D , E , β), the quality of hypolimnion temperature was greatly improved through
 382 calibration. This would seem to indicate that the quality of simulated hypolimnion temperature was improved
 383 through the improvement of epilimnion temperature simulations.

Table 4: Kendall's tau coefficients and p -values of CSS for model parameters values and drivers obtained from calibrated simulations (1959-2020) in respect to lakes geomorphological characteristics. The significance levels are represented as follows: *: $1.00e-02 < p\text{-value} \leq 5.00e-02$, **: $1.00e-03 < p\text{-value} \leq 1.00e-02$, *: $1.00e-04 < p\text{-value} \leq 1.00e-03$, ****: $p\text{-value} \leq 1.00e-04$. Otherwise, correlations are not significant ($p\text{-value} > 0.05$).**

	Maximal depth (m)	Surface area (km ²)	Altitude (m)	Latitude (°N)	Volume (m ³)
CSS_A	0.02	-0.1	0.14**	-0.08	-0.07
CSS_B	0.09	-0.04	0.14**	-0.14**	0.02
CSS_C	-0.04	-0.09	0.18***	-0.05	-0.1
CSS_D	-0.12*	0.02	-0.14**	0.06	-0.1
CSS_E	-0.01	-0.001	0.02	0.0003	-0.03
CSS_α	0.47****	0.07	0.4****	-0.23****	0.39****
CSS_β	0.16**	-0.12*	0.22****	-0.19***	0.05
CSS_{at_factor}	-0.25****	-0.14**	-0.13*	0.04	-0.28****
CSS_{sw_factor}	-0.22****	-0.06	-0.14**	0.06	-0.2****
CSS_{MAAT}	-0.09	-0.13**	0.13*	-0.02	-0.15**



384

Figure 5 : Composite scaled sensitivities (CSS) for each model parameter as a function of maximal depth.

385 7. Discussion and implications

386 Lakes are undeniably changing under climate change and long-term future projections show that the shifts in
 387 ecosystem functioning will continue with aggravated alterations (Woolway & Merchant, 2019). In particular, given
 388 the key role of lake water temperature in regulating ecosystem processes, its warming has become a response that
 389 is crucial to monitor, explore and understand. Hence, the importance of developing or adopting approaches, such
 390 as numerical models, that will provide long-term information about water temperature and allow us to understand
 391 the thermal response of lakes to climate change.

392 Here we used a semi-empirical model, the OKPLM, to simulate six decades of epilimnion and hypolimnion water
 393 temperatures in French lakes. In comparison to similar models, overall, the OKPLM provides acceptable
 394 estimations of water temperatures, with better results for epilimnion temperatures. The values of the RMSEs
 395 provided in Prats & Danis (2019) and obtained between OKPLM simulations and observations are comparable to
 396 values found in studies applying complex hydrodynamic lake models (Read et al., 2014; Fang et al., 2012). When
 397 using the default parameter values, the uncertainty associated with epilimnion temperature simulations was
 398 significantly related to all geomorphological characteristics however, it was especially strongly correlated to lake
 399 maximal depth. In contrast, the uncertainty in the hypolimnion simulations had a significant correlation solely with
 400 altitude and maximal depth. The importance of this correlation was especially noteworthy in the case of reservoirs
 401 located in low-altitude regions where uncertainties were the lowest. While the association between hypolimnion
 402 uncertainty and maximal depth exhibited only a weak correlation, the instances of highest uncertainties were
 403 predominantly found in reservoirs having maximal depths around 10 m. The correlations found between lakes
 404 geomorphological characteristics and simulations uncertainties suggests that there might be systematic biases in
 405 the definition of model parameters or in the forcing data. The calibration of model parameters significantly reduced
 406 the uncertainties yet, for hypolimnion temperatures, they remained considerably high and increased with depth
 407 especially in reservoirs.

408 The high levels of uncertainty found in reservoirs could be somewhat attributed to the lack of consideration of
 409 water level fluctuations in the model. In contrast to other lakes (e.g., natural lakes, artificial lakes and gravel pits)

410 reservoirs experience significant variations in their water level, which influences the heat budget and hence their
411 thermal regime. Therefore, even under similar meteorological conditions lakes and reservoirs could have different
412 thermal behaviors (Nowlin et al., 2004). In reservoirs, the discharge depth is a driver of thermal structure. Deep
413 discharges could contribute to warmer bottom waters (Carr et al., 2020) whereas in some cases if the reservoir is
414 shallow or if the discharge depth is not deep, it could demonstrate lake-like thermal behavior. This does not
415 necessarily mean that, in this case, the entire functioning of the reservoir resembles one of a natural lake; there are
416 still differences to consider (Detmer et al., 2022).

417 The application of the OKPLM should be made with caution given its performance and depending on the objective
418 of the study. The model does not take into account a complete set of meteorological forcing (e.g., with cloud cover,
419 relative humidity and wind speed and direction) or other variables (e.g., inflow and outflow rates or water level
420 fluctuations, inflow discharge depth and inflow temperature) that could influence the thermal structure of the
421 ecosystem (Yang et al., 2020; Carr et al., 2020). Furthermore, the OKPLM was parametrized for a specific set of
422 lakes with particular geomorphological characteristics. Thus, it would be advisable to apply the model over lakes
423 with similar characteristics. If the aim is to conduct a long-term regional or global study for studying general
424 patterns of climate change impacts over a large number of study sites, the utilization of semi-empirical models
425 such as the OKPLM is the most suitable choice. Although complex, deterministic or process-based models provide
426 a more accurate representation of thermal conditions, applying these models over several study sites and for long
427 periods is usually hindered by the scarcity of the required input data. The increased complexity of these models
428 (with reference to an increased number of model parameters) is beneficial for representing additional ecosystem
429 processes. Yet the greater number of model parameters, increases the sensitivity of models and demands more
430 calibration efforts (Lindenschmidt, 2006). Furthermore, a reduction in model errors is sometimes associated with
431 an increased complexity in model structure; however, this is not always consistent since a complex model does
432 not necessarily provide better estimations and thus lower errors than a simple model (Snowling and Kramer, 2001).

433 Our goal in publishing the present dataset is to expand knowledge about the water temperature of French lakes and
434 provide data, with enough details and reliability, that it could be implemented in different studies where water
435 temperature is implicated for understanding specific processes or interactions, in particular under climate change.
436 Hence the significance of the present findings. The present study, making use of a semi-empirical model to provide
437 long-term data about water temperature, was necessary for several reasons. Equipping a large number of lakes
438 with thermal sensors is challenging and labor-intensive, it comes with a high financial cost that is often not
439 available. Consequently, historical and even current water temperature datasets are often scarce, which can be
440 problematic for studying the impact of climate change, as it requires high frequency data over a long duration of
441 time for accurate analysis. In general, the higher the sampling frequency and duration, the better the data is suited
442 to estimate or analyze specific processes or warming trends. The sampling frequency and length of a dataset have
443 been shown to play a role in determining the accuracy of estimating warming trends where time series longer than
444 30 years seem to be the most appropriate (Gray et al., 2018). Although, the duration and frequency of a dataset
445 have a major role in reflecting accurate representations, their influence is scarcely addressed when it comes to
446 climate change studies related to warming trends in water temperature.

447 This dataset is very useful for climate change studies; it could be used for developing and analyzing several
448 temperature indicators (e.g., annual or seasonal maximal and minimal temperature values, temperature exceeding

449 certain thresholds with biological implications, etc.). Further, mixing and stratification dynamics are important to
450 characterize as they drive lake biogeochemistry. Among other processes, they influence the distribution of
451 nutrients, primary productivity and the composition of phytoplankton and zooplankton communities along the
452 water column (Judd et al., 2005). With the LakeTSim dataset, it is possible to classify the mixing regime of lakes
453 and investigate possible triggers of regime shifts.

454 **8. Data usage**

455 The LakeTSim dataset comprises water temperature simulations for natural lakes ($n = 54$), reservoirs ($n = 302$),
456 gravel pits ($n = 7$), and other artificial lakes (e.g., ponds and quarry lakes, $n = 38$). The simulations are for both the
457 epi- and hypolimnion. Lakes that are fully mixed throughout the year (typically, shallower lakes) have the same
458 temperature value for both layers. More generally, the delta of temperature can be used to calculate mixing regimes
459 (Sharaf et al., in prep.).

460 The lakes in the dataset were selected because they are monitored as part of the European Water Framework
461 Directive (Directive 2000/60/EC). The majority of the 401 lakes are non-natural and some were only created after
462 1959 (i.e., the start of our simulations). We compiled the initial filling years for 282 of these 347 non-natural lakes
463 (269 reservoirs and 13 artificial lakes, Figure A8 in Appendix A) in Table S1 (see Supplement) to be used as a
464 companion dataset to LakeTSim. The filling years were sourced from <https://www.barrages-cfbr.eu> for 179 of the
465 lakes and from the PLAN_DEAU database for 103 of the lakes; the information was not available for 33 reservoirs,
466 7 gravel pits and 25 other artificial lakes of the LakeTSim dataset.

467 The median filling date was 1962 and 67% of the lakes with known filling dates were filled by 1980. While the
468 complete simulations ranging from 1959 to 2020 can also be used as theoretical lake temperature for comparison
469 across similar periods, we recommend that users of LakeTSim data for reservoir and artificial lake simulations
470 consider the initial filling dates provided in Table S1 to filter out years from the simulations during which lakes
471 were not filled yet.

472 Additionally, users should be aware that some reservoirs might be drained completely at certain intervals (e.g.,
473 every 10 years) for maintenance and inspection purposes. Finally, as mentioned in the discussion, some of the
474 lakes in the dataset experience artificial (e.g., in reservoirs) or natural (e.g., in some smaller ponds) water level
475 fluctuations, and potential intermittent dry-periods lasting weeks or months; none of these hydrological processes
476 are accounted for in the simulations.

477 **9. Code availability**

478 The respective codes for the “CUSPY” (Prats-Rodríguez and Danis, 2023a) and “OKPLM” (Prats-Rodríguez and
479 Danis, 2023b) packages, which can be used to conduct sensitivity and uncertainty analysis and to run the OKP
480 Lake Model, are available at <https://github.com/inrae/ALAMODE-cuspy> and
481 <https://github.com/inrae/ALAMODE-okp> as well as ZENODO.

482 **10. Data availability**

483 The LakeTSim dataset (Sharaf et al., 2023) for epilimnion and hypolimnion water temperature simulations and
484 supporting information are available at [doi:10.57745/OF9WXR](https://doi.org/10.57745/OF9WXR). The file “00_Data_description.txt” contains a
485 description of the dataset. The geographical (longitude and latitude) and morphological (surface area, volume and

486 maximal depth) data for the 401 lakes are presented in the file “01_Lake_data.txt” in addition to the name, type,
487 altitude and the identification code for each lake. The data are located in two main folders: “02_Temperature_data”
488 containing daily epilimnion (tepi) and hypolimnion (thyp) temperatures simulated with the OKPLM and
489 “03_Uncertainty_data” containing daily tepi and thyp uncertainties. In each folder, the data for temperature
490 simulations and their uncertainties are presented in text files available in the folders
491 “00_LakeTSim_SAFRAN_OKPdefault_data”, “01_LakeTSim_SAFRAN_OKPcalibrated_data”,
492 “02_LakeTSim_S2M_OKPdefault_data” and “03_LakeTSim_S2M_OKPcalibrated_data”. The name of each file
493 within these folders includes the identification code of the lake. From 2024, the data will be visible from a
494 dashboard. The link to the dashboard will be accessible from data.ecla.inrae.fr.

495 **11. Conclusions**

496 We present the LakeTSim dataset and the semi-empirical OKP Lake Model for simulating water temperature in
497 Lakes. We applied the model over a set of 401 French lakes for the period 1959-2020 to derive daily simulations
498 of epilimnion and hypolimnion water temperatures, here referred to as the LakeTSim dataset. Previous efforts to
499 assess the model’s performance show an overall acceptable representation of epilimnion and hypolimnion
500 temperatures when compared to in situ measurements. The uncertainty analysis of simulations demonstrates that
501 higher uncertainties are found for, by order of relative importance: (1) default simulations, (2) hypolimnion
502 compared to epilimnion temperatures and, (3) deep lakes, in particular reservoirs (maximal depth greater than 10
503 m for epilimnion temperature and around 10 m for hypolimnion temperature simulated with default model
504 parameters). Although the calibration significantly decreases the uncertainties related to both the epilimnion and
505 hypolimnion, in some cases they are still considerable in the hypolimnion. Based on these results and if enough
506 observation data are available, optimally we recommend the use of the OKPLM for shallow (maximal depth < 8
507 m) lakes with calibrated model parameters. However, if applied in its default or even calibrated configuration over
508 deep lakes, one should be aware of the presented limitations and address them in the analysis. The LakeTSim
509 dataset is valuable for assessing the impact of climate change on lakes thermal functioning, which is often hindered
510 by the lack of water temperature observations. The present dataset will provide new insights about the thermal
511 behavior of French lakes, which can provide useful context for stakeholders as they design management strategies
512 in a context of climate change.

513

514

515

516

517

518

519

520

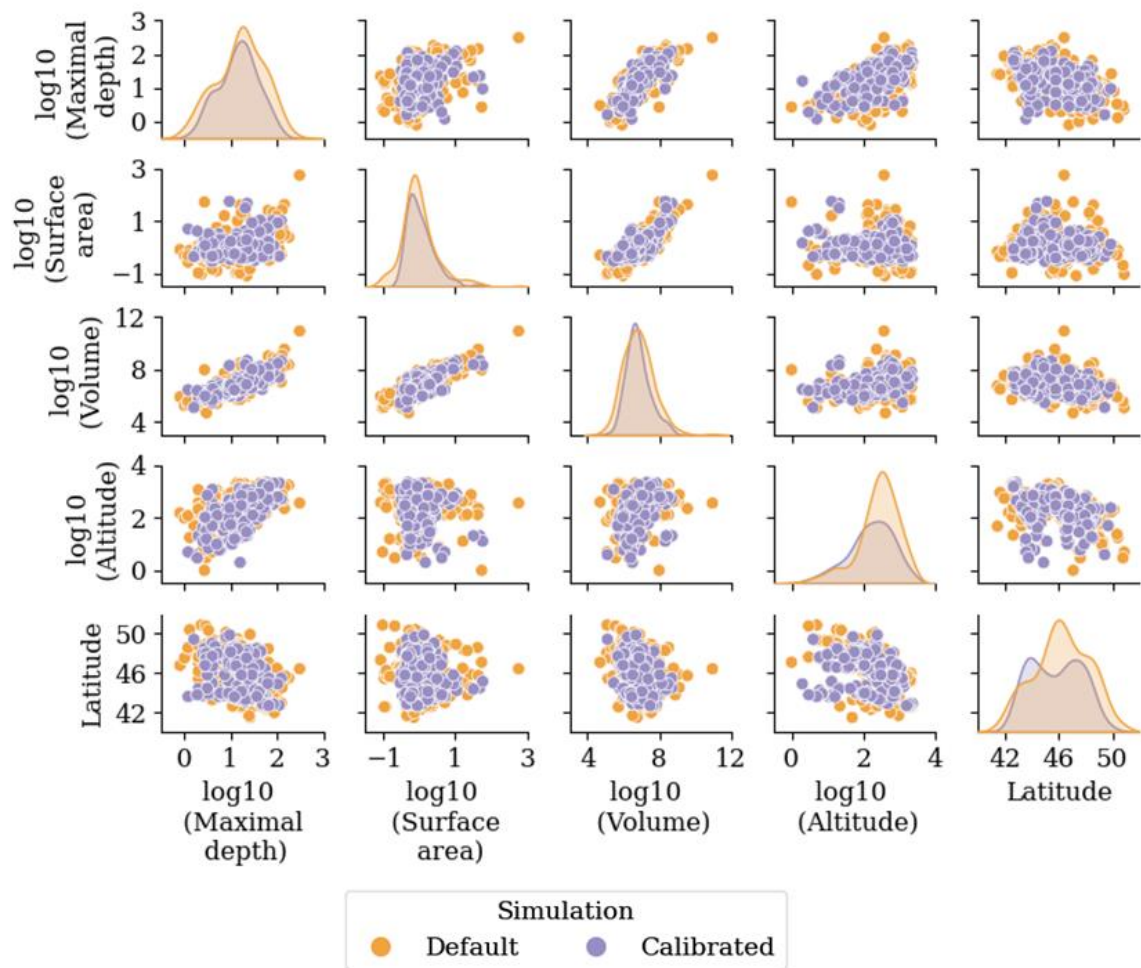


Figure A1: Scatter plots of lakes ($n = 401$) geomorphological characteristics: Maximal depth (m), Surface area (km²), volume (m³), altitude (m) and latitude (°N).

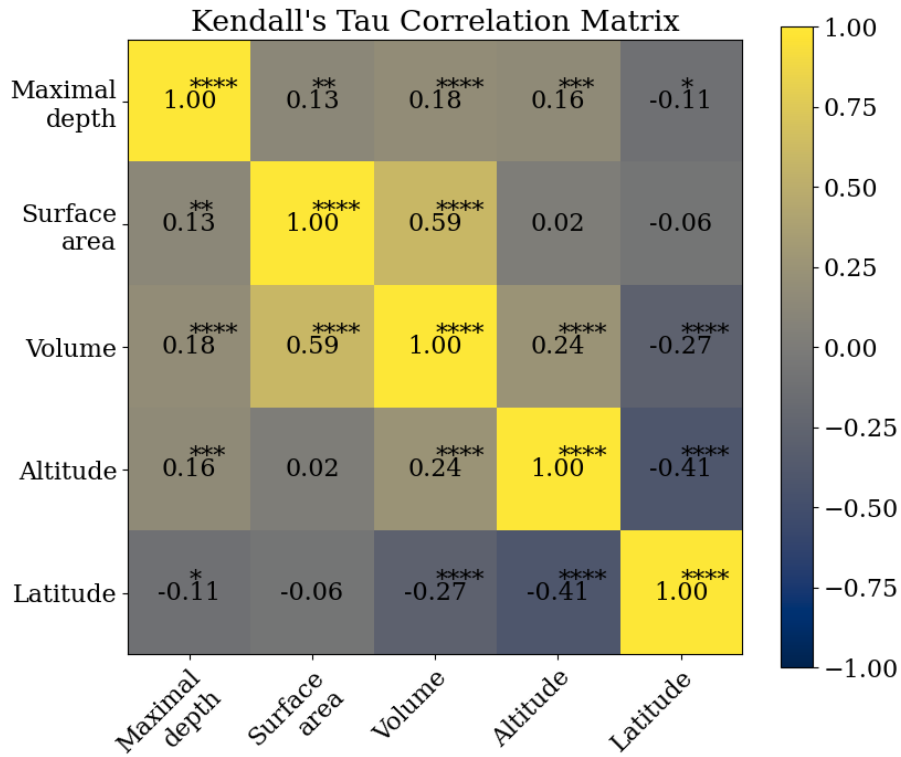


Figure A2: Kendall's tau correlation matrix of the geomorphological characteristics of lakes simulated in "default" mode ($n = 231$): Maximal depth (m), Surface area (km^2), volume (m^3), altitude (m) and latitude ($^\circ\text{N}$). The significance levels are represented as follows: *: $1.00\text{e-}02 < p\text{-value} \leq 5.00\text{e-}02$, **: $1.00\text{e-}03 < p\text{-value} \leq 1.00\text{e-}02$, ***: $1.00\text{e-}04 < p\text{-value} \leq 1.00\text{e-}03$, ****: $p\text{-value} \leq 1.00\text{e-}04$. Otherwise, correlations are not significant ($p\text{-value} > 0.05$).

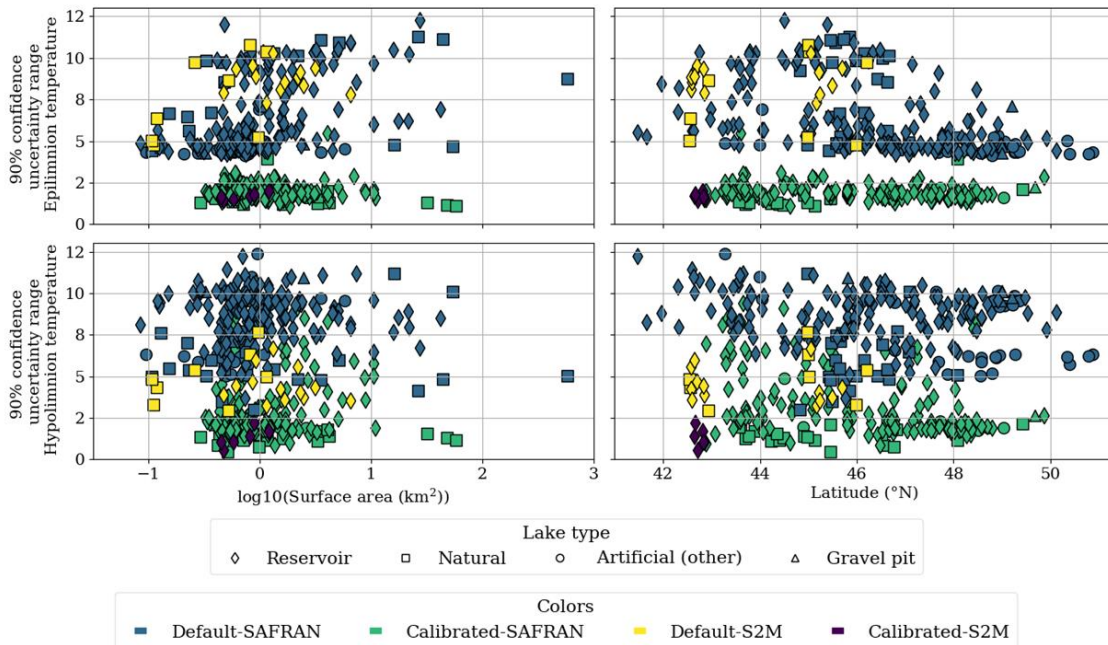


Figure A3: Average 90% confidence uncertainty range for epilimnion (top panel) and hypolimnion (bottom panel) temperatures in calibrated ($n = 170$) and default ($n = 231$) simulations for the period 1959-2020 as a function of surface area (km^2) and latitude ($^\circ\text{N}$).

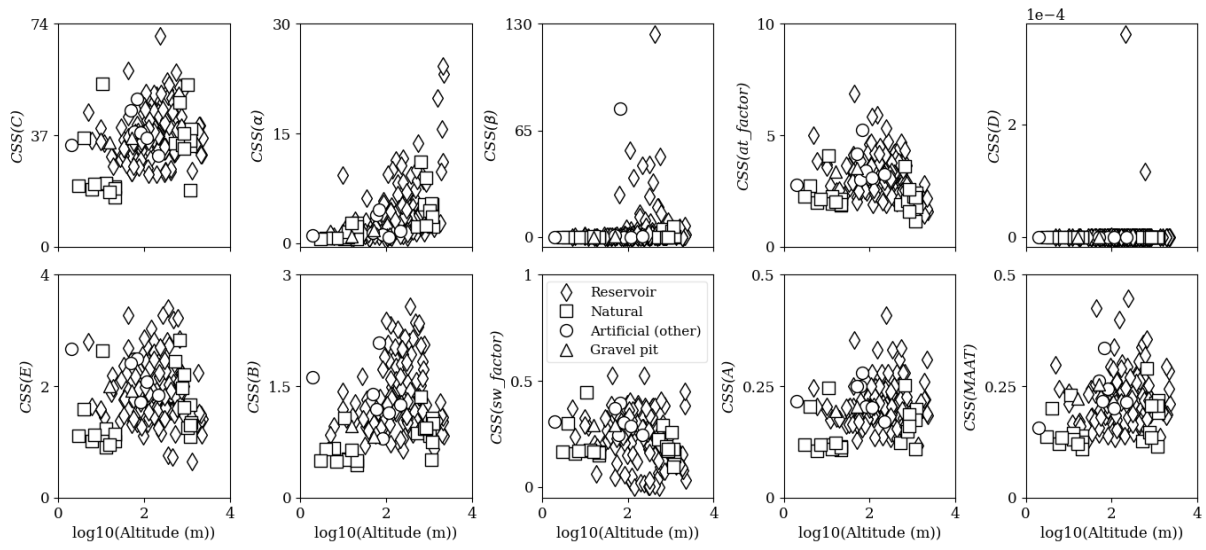


Figure A4: Composite scaled sensitivities (CSS) for each model parameter as a function of altitude.

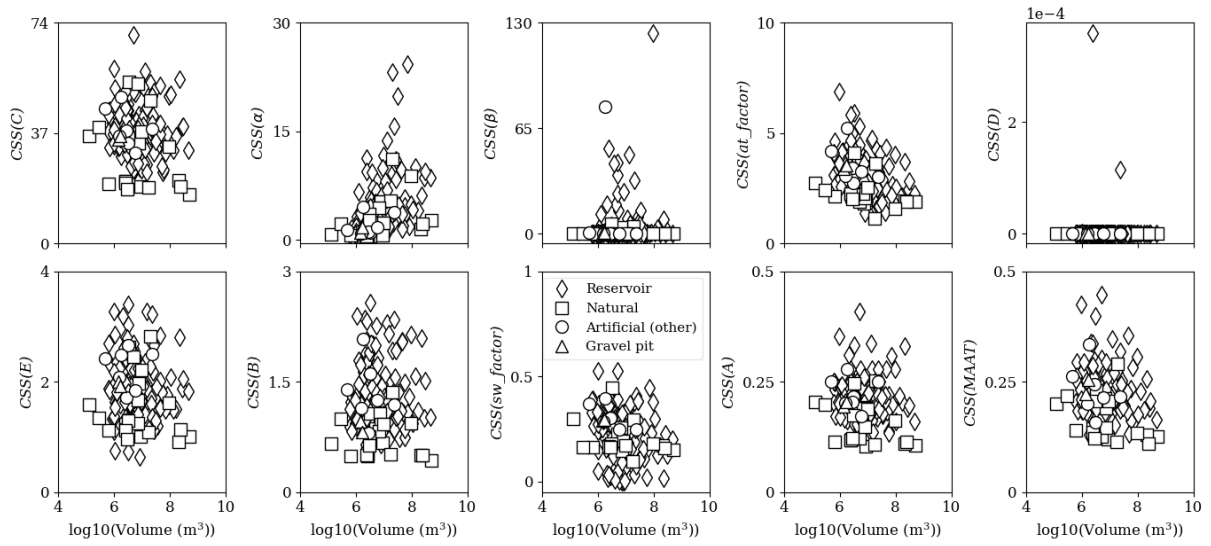


Figure A5: Composite scaled sensitivities (CSS) for each model parameter as a function of volume.

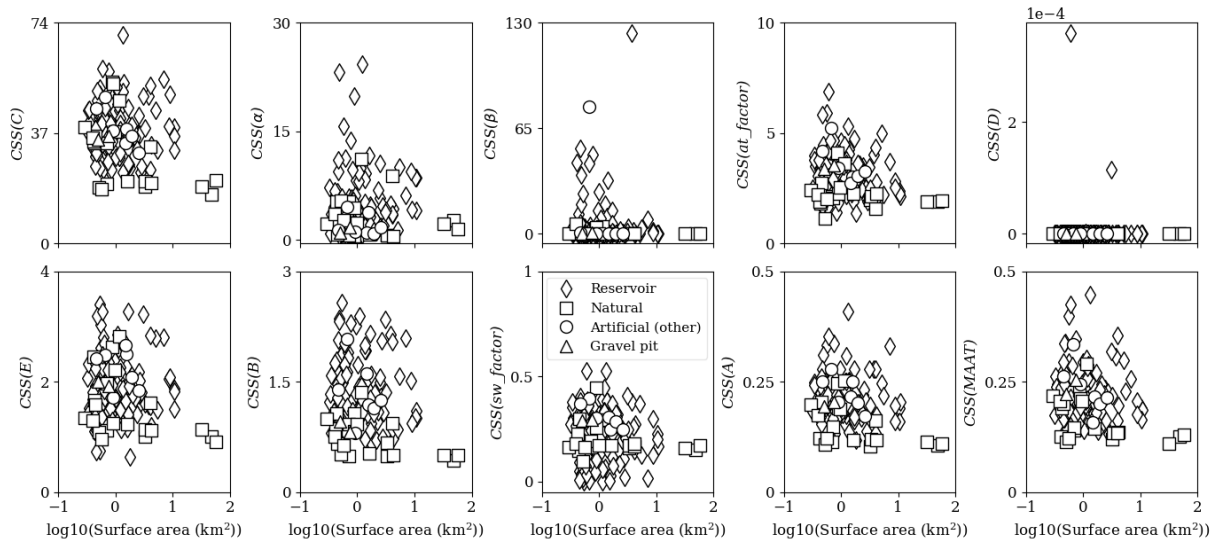


Figure A6: Composite scaled sensitivities (CSS) for each model parameter as a function of surface area.

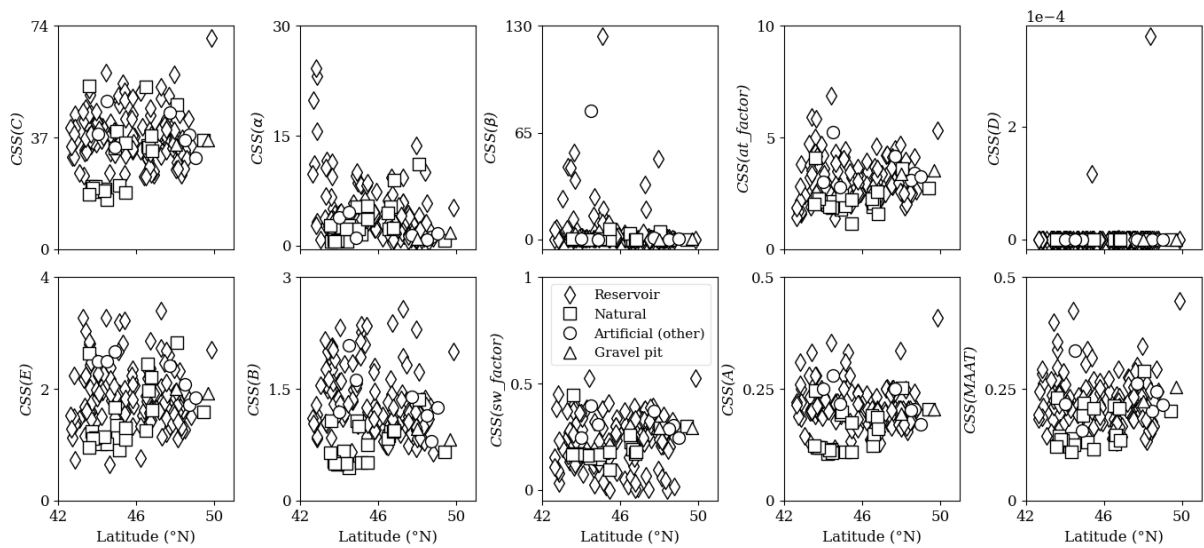
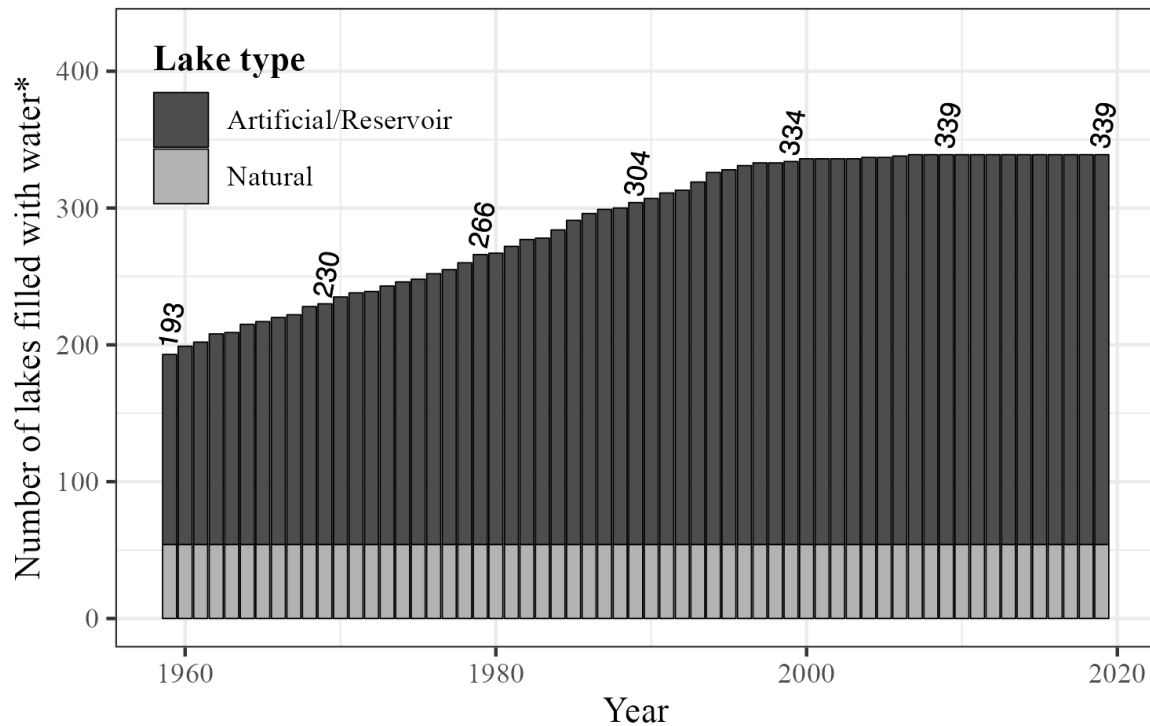


Figure A7: Composite scaled sensitivities (CSS) for each model parameter as a function of latitude.



* 7 gravel pits, 33 reservoirs & 25 other artificial lakes with no information on filling year.

Figure A8: Distribution of initial filling years for lakes (e.g., reservoirs, gravel pits and other artificial lakes) of the LakeTSim dataset.

523 **13. Author contributions**

524 NS wrote the original manuscript with input from JP and PAD. NS, JP and PAD discussed the results. JP developed
 525 and carried out the implementation of the OKP Lake Model and the uncertainties computation in ALAMODE. JP
 526 and NS performed the simulations and provided uncertainty analysis results with SAFRAN and S2M data
 527 respectively. JP and NS implemented respectively the integration of SAFRAN and S2M data in ALAMODE. NS
 528 prepared the LakeTSim dataset. JP and NS provided the uncertainty and sensitivity analysis. PAD designed,
 529 contributed and supervised the implementation of S2M data in ALAMODE for forcing the OKPLM when
 530 simulating high altitude lakes. PAD supervised the findings of this work. RB proposed and contributed to the
 531 integration of the data consisting of initial filling dates of reservoirs and other artificial lakes in the manuscript.
 532 NR and TT supervised and contributed to the implementation of simulation results in the database. NR processed
 533 S2M data and compiled the data for initial filling years of reservoirs and other artificial lakes. NR and TT prepared
 534 the doi for the LakeTSim dataset. TP conducted the fieldwork for the monitoring, acquisition and verification of
 535 in situ temperature data. All authors reviewed, edited and approved the final paper.

536 **14. Competing interests**

537 The authors declare that they have no conflict of interest.

538 **15. Acknowledgments**

539 The authors thank Météo-France for providing SAFRAN and S2M meteorological data, Matthieu Vernay for his
540 feedback on the utilization of S2M data and the “Réseau Lacs Sentinelles” for providing bathymetry data for
541 mountain lakes.

542 **16. Financial support**

543 The authors were supported by OFB (Office Français de la Biodiversité), SEGULA Technologies, INRAE (Institut
544 National de Recherche pour l’Agriculture, l’Alimentation et l’environnement) and Pôle R&D ECLA
545 (ECosystèmes LAcustres).

546 **17. References**

- 547 Adrian, R., O’Reilly, C. M., Zagarese, H., Baines, S. B., Hessen, D. O., Keller, W., Livingstone, D. M.,
548 Sommaruga, R., Straile, D., Van Donk, E., Weyhenmeyer, G. A., and Winder, M.: Lakes as sentinels of climate
549 change, *Limnol. Oceanogr.*, 54, 2283–2297, https://doi.org/10.4319/lo.2009.54.6_part_2.2283, 2009.
- 550 Allan, M. G., Hamilton, D. P., Trolle, D., Muraoka, K., and McBride, C.: Spatial heterogeneity in geothermally-
551 influenced lakes derived from atmospherically corrected Landsat thermal imagery and three-dimensional
552 hydrodynamic modelling, *Int. J. Appl. Earth Obs. Geoinf.*, 50, 106–116, <https://doi.org/10.1016/j.jag.2016.03.006>,
553 2016.
- 554 Babbar-Sebens, M., Li, L., Song, K., and Xie, S.: On the Use of Landsat-5 TM Satellite for Assimilating Water
555 Temperature Observations in 3D Hydrodynamic Model of Small Inland Reservoir in Midwestern US, *Adv.*
556 *Remote Sens.*, 02, 214–227, <https://doi.org/10.4236/ars.2013.23024>, 2013.
- 557 Carr, M. K., Sadeghian, A., Lindenschmidt, K. E., Rinke, K., and Morales-Marin, L.: Impacts of Varying Dam
558 Outflow Elevations on Water Temperature, Dissolved Oxygen, and Nutrient Distributions in a Large Prairie
559 Reservoir, *Environ. Eng. Sci.*, 37, 78–97, <https://doi.org/10.1089/ees.2019.0146>, 2020.
- 560 Danis, P.: Rapport d ’avancement sur les outils de modélisation thermique, 1–8 pp., <https://doi.org/hal-03253847>,
561 2020.
- 562 Daufresne, M., Lengfellner, K., and Sommer, U.: Global warming benefits the small in aquatic ecosystems, *Proc.*
563 *Natl. Acad. Sci.*, 106, 12788–12793, <https://doi.org/10.1073/pnas.0902080106>, 2009.
- 564 Detmer, T. M., Parkos, J. J., and Wahl, D. H.: Long-term data show effects of atmospheric temperature anomaly
565 and reservoir size on water temperature, thermal structure, and dissolved oxygen, *Aquat. Sci.*, 84, 1–13,
566 <https://doi.org/10.1007/s00027-021-00835-2>, 2022.
- 567 Durand, Y., Brun, E., Merindol, L., Guyomarc’h, G., Lesaffre, B., and Martin, E.: A meteorological estimation of
568 relevant parameters for snow models, *Ann. Glaciol.*, 18, 65–71, <https://doi.org/10.3189/S0260305500011277>,
569 1993.
- 570 Ely, D. M.: Analysis of Sensitivity of Simulated Recharge to Selected Parameters for Seven Watersheds Modeled
571 Using the Precipitation-Runoff Modeling System, U.S. Geological Survey Scientific Investigations Rep, 21 pp.,
572 2006.
- 573 Fang, X., Alam, S. R., Stefan, H. G., Jiang, L., Jacobson, P. C., and Pereira, D. L.: Simulations of water quality
574 and oxythermal cisco habitat in Minnesota lakes under past and future climate scenarios, *Water Qual. Res. J.*
575 *Canada*, 47, 375–388, <https://doi.org/10.2166/wqrjc.2012.031>, 2012.
- 576 Gray, D. K., Hampton, S. E., O’Reilly, C. M., Sharma, S., and Cohen, R. S.: How do data collection and processing
577 methods impact the accuracy of long-term trend estimation in lake surface-water temperatures?, *Limnol.*
578 *Oceanogr. Methods*, 16, 504–515, <https://doi.org/10.1002/lom3.10262>, 2018.
- 579 Griffith, A. W. and Gobler, C. J.: Harmful algal blooms: A climate change co-stressor in marine and freshwater
580 ecosystems, *Harmful Algae*, 91, 101590, <https://doi.org/10.1016/j.hal.2019.03.008>, 2020.
- 581 Halverson, G. H., Lee, C. M., Hestir, E. L., Hulley, G. C., Cawse-Nicholson, K., Hook, S. J., Bergamaschi, B. A.,
582 Acuña, S., Tufillaro, N. B., Radocinski, R. G., Rivera, G., and Sommer, T. R.: Decline in Thermal Habitat
583 Conditions for the Endangered Delta Smelt as Seen from Landsat Satellites (1985–2019), *Environ. Sci. Technol.*,

584 56, 185–193, <https://doi.org/10.1021/acs.est.1c02837>, 2022.

585 Havens, K. and Jeppesen, E.: Ecological responses of lakes to climate change, *Water*, 10, 917,
586 <https://doi.org/10.3390/w10070917>, 2018.

587 Hill, M. C.: Methods and guidelines for effective model calibration: U.S. Geological Survey Water-Resources
588 Investigations Report 98-4005, 90 pp., <https://doi.org/10.3133/wri984005>, 1998.

589 Hipsey, M. R., Bruce, L. C., Boon, C., Busch, B., Carey, C. C., Hamilton, D. P., Hanson, P. C., Read, J. S., De
590 Sousa, E., Weber, M., and Winslow, L. A.: A General Lake Model (GLM 3.0) for linking with high-frequency
591 sensor data from the Global Lake Ecological Observatory Network (GLEON), *Geosci. Model Dev.*, 12, 473–523,
592 <https://doi.org/10.5194/gmd-12-473-2019>, 2019.

593 Janssen, A. B. G., Hilt, S., Kosten, S., de Klein, J. J. M., Paerl, H. W., and Van de Waal, D. B.: Shifting states,
594 shifting services: Linking regime shifts to changes in ecosystem services of shallow lakes, *Freshw. Biol.*, 66, 1–
595 12, <https://doi.org/10.1111/fwb.13582>, 2021.

596 Javaheri, A., Babbar-Sebens, M., and Miller, R. N.: From skin to bulk: An adjustment technique for assimilation
597 of satellite-derived temperature observations in numerical models of small inland water bodies, *Adv. Water
598 Resour.*, 92, 284–298, <https://doi.org/10.1016/j.advwatres.2016.03.012>, 2016.

599 Judd, K. E., Adams, H. E., Bosch, N. S., Kostrzewski, J. M., Scott, C. E., Schultz, B. M., Wang, D. H., and Kling,
600 G. W.: A case history: Effects of mixing regime on nutrient dynamics and community structure in third sister lake,
601 michigan during late winter and early spring 2003, *Lake Reserv. Manag.*, 21, 316–329,
602 <https://doi.org/10.1080/07438140509354437>, 2005.

603 Kettle, H., Thompson, R., Anderson, N. J., and Livingstone, D. M.: Empirical modeling of summer lake surface
604 temperatures in southwest Greenland, *Limnol. Oceanogr.*, 49, 271–282,
605 <https://doi.org/10.4319/lo.2004.49.1.0271>, 2004.

606 Kharouba, H. M., Ehrlén, J., Gelman, A., Bolmgren, K., Allen, J. M., Travers, S. E., and Wolkovich, E. M.: Global
607 shifts in the phenological synchrony of species interactions over recent decades, *Proc. Natl. Acad. Sci. U. S. A.*,
608 115, 5211–5216, <https://doi.org/10.1073/pnas.1714511115>, 2018.

609 Kim, J., Seo, D., Jang, M., and Kim, J.: Augmentation of limited input data using an artificial neural network
610 method to improve the accuracy of water quality modeling in a large lake, *J. Hydrol.*, 602, 126817,
611 <https://doi.org/10.1016/j.jhydrol.2021.126817>, 2021.

612 Layden, A., Merchant, C., and Maccallum, S.: Global climatology of surface water temperatures of large lakes by
613 remote sensing, *Int. J. Climatol.*, 35, 4464–4479, <https://doi.org/10.1002/joc.4299>, 2015.

614 Lind, L., Eckstein, R. L., and Relyea, R. A.: Direct and indirect effects of climate change on distribution and
615 community composition of macrophytes in lentic systems, *Biol. Rev.*, 1686, 1677–1690,
616 <https://doi.org/10.1111/brv.12858>, 2022.

617 Lindenschmidt, K. E.: The effect of complexity on parameter sensitivity and model uncertainty in river water
618 quality modelling, *Ecol. Modell.*, 190, 72–86, <https://doi.org/10.1016/j.ecolmodel.2005.04.016>, 2006.

619 Mironov, D. V.: Parameterization of lakes in numerical weather prediction: Description of a lake model,
620 *Encyclopedic Dictionary of Archaeology*, Offenbach, Germany: DWD, 2008.

621 Nouchi, V., Kutser, T., Wüest, A., Müller, B., Odermatt, D., Baracchini, T., and Bouffard, D.: Resolving
622 biogeochemical processes in lakes using remote sensing, *Aquat. Sci.*, 81, 1–13, <https://doi.org/10.1007/s00027-019-0626-3>, 2019.

624 Nowlin, W. H., Davies, J. M., Nordin, R. N., and Mazumder, A.: Effects of water level fluctuation and short-term
625 climate variation on thermal and stratification regimes of a British Columbia reservoir and lake, *Lake Reserv.
626 Manag.*, 20, 91–109, <https://doi.org/10.1080/07438140409354354>, 2004.

627 Ottosson, F. and Abrahamsson, O.: Presentation and analysis of a model simulating epilimnetic and hypolimnetic
628 temperatures in lakes, *Ecol. Modell.*, 110, 233–253, [https://doi.org/10.1016/S0304-3800\(98\)00067-2](https://doi.org/10.1016/S0304-3800(98)00067-2), 1998.

629 Piccolroaz, S., Toffolon, M., and Majone, B.: A simple lumped model to convert air temperature into surface water
630 temperature in lakes, *Hydrol. Earth Syst. Sci.*, 17, 3323–3338, <https://doi.org/10.5194/hess-17-3323-2013>, 2013.

631 Piccolroaz, S., Woolway, R. I., and Merchant, C. J.: Global reconstruction of twentieth century lake surface water

- 632 temperature reveals different warming trends depending on the climatic zone, *Clim. Change*, 160, 427–442,
633 <https://doi.org/10.1007/s10584-020-02663-z>, 2020.
- 634 Poeter, E. P. and Hill, M. C.: Inverse models: A necessary next step in ground-water modeling, *Groundwater*, 35,
635 250–260, 1997.
- 636 Prats-Rodríguez, J. and Danis, P.-A.: inrae/ALAMODE-cuspy: cuspy v1.0,
637 <https://doi.org/10.5281/ZENODO.7585606>, 2023a.
- 638 Prats-Rodríguez, J. and Danis, P.-A.: inrae/ALAMODE-okp: okplm v1.0,
639 <https://doi.org/10.5281/ZENODO.7564750>, 2023b.
- 640 Prats, J. and Danis, P.-A.: Optimisation du réseau national de suivi pérenne in situ de la température des plans
641 d'eau : apport de la modélisation et des données satellitaires, [Rapport Rech. irstea, 93, <https://doi.org/hal-02602604>, 2015.
- 643 Prats, J. and Danis, P. A.: An epilimnion and hypolimnion temperature model based on air temperature and lake
644 characteristics, *Knowl. Manag. Aquat. Ecosyst.*, 8, <https://doi.org/10.1051/kmae/2019001>, 2019.
- 645 Prats, J., Reynaud, N., Rebière, D., Peroux, T., Tormos, T., and Danis, P. A.: LakeSST: Lake Skin Surface
646 Temperature in French inland water bodies for 1999-2016 from Landsat archives, *Earth Syst. Sci. Data*, 10, 727–
647 743, <https://doi.org/10.5194/essd-10-727-2018>, 2018.
- 648 Read, J. S., Winslow, L. A., Hansen, G. J. A., Van Den Hoek, J., Hanson, P. C., Bruce, L. C., and Markfort, C. D.:
649 Simulating 2368 temperate lakes reveals weak coherence in stratification phenology, *Ecol. Modell.*, 291, 142–150,
650 <https://doi.org/10.1016/j.ecolmodel.2014.07.029>, 2014.
- 651 Rimet, F., Anneville, O., Barbet, D., Chardon, C., Crépin, L., Domaizon, I., Dorioz, J. M., Espinat, L., Frossard,
652 V., Guillard, J., Goulon, C., Hamelet, V., Hustache, J. C., Jacquet, S., Lainé, L., Montuelle, B., Perney, P., Quetin,
653 P., Rasconi, S., Schellenberger, A., Tran-Khac, V., and Monet, G.: The Observatory on LAKes (OLA) database:
654 Sixty years of environmental data accessible to the public, *J. Limnol.*, 79, 164–178,
655 <https://doi.org/10.4081/jlimnol.2020.1944>, 2020.
- 656 Schaeffer, B. A., Iames, J., Dwyer, J., Urquhart, E., Salls, W., Rover, J., and Seegers, B.: An initial validation of
657 Landsat 5 and 7 derived surface water temperature for U.S. lakes, reservoirs, and estuaries, *Int. J. Remote Sens.*,
658 39, 7789–7805, <https://doi.org/10.1080/01431161.2018.1471545>, 2018.
- 659 Sharaf, N., Fadel, A., Bresciani, M., Giardino, C., Lemaire, B. J., Slim, K., Faour, G., and Vinçon-Leite, B.: Lake
660 surface temperature retrieval from Landsat-8 and retrospective analysis in Karaoun Reservoir, Lebanon, *J. Appl.*
661 *Remote Sens.*, 13, 1, <https://doi.org/10.1117/1.jrs.13.044505>, 2019.
- 662 Sharaf, N., Lemaire, B. J., Fadel, A., Slim, K., and Vinçon-Leite, B.: Assessing the thermal regime of poorly
663 monitored reservoirs with a combined satellite and three-dimensional modeling approach, *Int. Waters*, 11, 302–
664 314, <https://doi.org/10.1080/20442041.2021.1913937>, 2021.
- 665 Sharaf, N., Prats, J., Reynaud, N., Tormos, T., Bruel, R., Peroux, T., and Danis, P. A.: LakeTSim (Lake
666 Temperature Simulations), *Rech. Data Gouv*, <https://doi.org/doi:10.57745/OF9WXR>, 2023.
- 667 Sharma, S., Walker, S. C., and Jackson, D. A.: Empirical modelling of lake water-temperature relationships: A
668 comparison of approaches, *Freshw. Biol.*, 53, 897–911, <https://doi.org/10.1111/j.1365-2427.2008.01943.x>, 2008.
- 669 Sharma, S., Gray, D. K., Read, J. S., O'Reilly, C. M., Schneider, P., Quadrat, A., Gries, C., Stefanoff, S., Hampton,
670 S. E., Hook, S., Lenters, J. D., Livingstone, D. M., McIntyre, P. B., Adrian, R., Allan, M. G., Anneville, O., Arvola,
671 L., Austin, J., Bailey, J., Baron, J. S., Brookes, J., Chen, Y., Daly, R., Dokulil, M., Dong, B., Ewing, K., De Eyto,
672 E., Hamilton, D., Havens, K., Haydon, S., Hetzenauer, H., Heneberry, J., Hetherington, A. L., Higgins, S. N.,
673 Hixson, E., Izmet'eva, L. R., Jones, B. M., Kangur, K., Kasprzak, P., Köster, O., Kraemer, B. M., Kumagai, M.,
674 Kuusisto, E., Leshkevich, G., May, L., MacIntyre, S., Müller-Navarra, D., Naumenko, M., Noges, P., Noges, T.,
675 Niederhauser, P., North, R. P., Paterson, A. M., Plisnier, P. D., Rigosi, A., Rimmer, A., Rogora, M., Rudstam, L.,
676 Rusak, J. A., Salmaso, N., Samal, N. R., Schindler, D. E., Schladow, G., Schmidt, S. R., Schultz, T., Silow, E. A.,
677 Straile, D., Teubner, K., Verburg, P., Voutilainen, A., Watkinson, A., Weyhenmeyer, G. A., Williamson, C. E.,
678 and Woo, K. H.: A global database of lake surface temperatures collected by in situ and satellite methods from
679 1985-2009, *Sci. Data*, 2, 1–19, <https://doi.org/10.1038/sdata.2015.8>, 2015.
- 680 Shatwell, T., Thiery, W., and Kirillin, G.: Future projections of temperature and mixing regime of European
681 temperate lakes, *Hydrol. Earth Syst. Sci.*, 23, 1533–1551, <https://doi.org/10.5194/hess-23-1533-2019>, 2019.

682 Snowling, S. D. and Kramer, J. R.: Evaluating modelling uncertainty for model selection, *Ecol. Modell.*, 138, 17–
683 30, [https://doi.org/10.1016/S0304-3800\(00\)00390-2](https://doi.org/10.1016/S0304-3800(00)00390-2), 2001.

684 Toffolon, M., Piccolroaz, S., Majone, B., Soja, A. M., Peeters, F., Schmid, M., and Wüest, A.: Prediction of surface
685 temperature in lakes with different morphology using air temperature, *Limnol. Oceanogr.*, 59, 2185–2202,
686 <https://doi.org/10.4319/lo.2014.59.6.2185>, 2014.

687 Vernay, M., Lafaysse, M., Mérindol, L., Giraud, G., and Morin, S.: Ensemble forecasting of snowpack conditions
688 and avalanche hazard, *Cold Reg. Sci. Technol.*, 120, 251–262, <https://doi.org/10.1016/j.coldregions.2015.04.010>,
689 2015.

690 Vernay, M., Lafaysse, M., Monteiro, D., Hagenmuller, P., Nheili, R., Samacoïts, R., Verfaillie, D., and Morin, S.:
691 The S2M meteorological and snow cover reanalysis over the French mountainous areas: description and evaluation
692 (1958-2021), *Earth Syst. Sci. Data*, 14, 1707–1733, <https://doi.org/10.5194/essd-14-1707-2022>, 2022.

693 White, J. T., Fienen, M. N., and Doherty, J. E.: A python framework for environmental model uncertainty analysis,
694 *Environ. Model. Softw.*, 85, 217–228, <https://doi.org/10.1016/j.envsoft.2016.08.017>, 2016.

695 White, J. T., Hunt, R. J., Fienen, M. N., Doherty, J. E., and Survey, U. S. G.: Approaches to highly parameterized
696 inversion: PEST++ Version 5, a software suite for parameter estimation, uncertainty analysis, management
697 optimization and sensitivity analysis:, *U.S. Geological Survey Techniques and Methods 7C26*, 52 pp.,
698 <https://doi.org/10.3133/tm7C26>, 2020.

699 Woolway, R. I. and Merchant, C. J.: Worldwide alteration of lake mixing regimes in response to climate change,
700 *Nat. Geosci.*, 12, 271–276, <https://doi.org/10.1038/s41561-019-0322-x>, 2019.

701 Woolway, R. I., Sharma, S., and Smol, J. P.: Lakes in Hot Water : The Impacts of a Changing Climate on Aquatic
702 Ecosystems, *Bioscience*, <https://doi.org/10.1093/biosci/biac052>, 2022.

703 Yang, K., Yu, Z., Luo, Y., Yang, Y., Zhao, L., and Zhou, X.: Spatial and temporal variations in the relationship
704 between lake water surface temperatures and water quality - A case study of Dianchi Lake, *Sci. Total Environ.*,
705 624, 859–871, <https://doi.org/10.1016/j.scitotenv.2017.12.119>, 2018.

706 Yang, K., Yu, Z., and Luo, Y.: Analysis on driving factors of lake surface water temperature for major lakes in
707 Yunnan-Guizhou Plateau, *Water Res.*, 184, 116018, <https://doi.org/10.1016/j.watres.2020.116018>, 2020.

708